An Assessment of the Current WAAS Ionospheric Correction Algorithm in the South American Region

ATTILA KOMJATHY, LAWRENCE SPARKS, ANTHONY J. MANNUCCI, and XIAOQING PI
NASA Jet Propulsion Laboratory/California Institute of Technology, Pasadena, California

Received September 2002; Revised July 2003

ABSTRACT: *The Federal Aviation Administration's (FAA) Wide Area Augmentation System (WAAS) for civil aircraft navigation is focused primarily on the conterminous United States (CONUS). In this paper, based on a limited dataset, we assess WAAS's planar fit algorithm in the equatorial region, where the spatial gradients and the absolute slant total electron content (TEC) are known to be the highest in the world. We found that in Brazil, the dominant error source for the WAAS planar fit algorithm is the inherent spatial variability of the equatorial ionosphere, with ionospheric slant range delay residuals as high as 15 m and root-mean-square (RMS) residuals for the quiet day of 1.9 m. This compares with a maximum residual of 2 m in CONUS and 0.5 m RMS. We discovered that ionospheric gradients in Brazil are at the 2 m over 100 km level. In contrast with results obtained for CONUS, we found that a major ionospheric storm had a small impact on the planar fit residuals in Brazil.*

INTRODUCTION

The Wide-Area Augmentation System (WAAS) developed for the conterminous United States (CONUS) is only one of several space-based augmentation systems (SBASs) under consideration worldwide. Other SBAS developments are under way in Europe, Japan, India, and Brazil.

Relatively benign ionospheric conditions in the midlatitude CONUS region are compatible with accurate ionospheric range corrections for WAAS. Providing ionospheric corrections for Brazil is significantly more challenging, since ionospheric range delays and range delay spatial gradients are among the largest in the world in the absence of ionospheric storms (during infrequent ionospheric storms, even midlatitude regions present challenging conditions). In summary, the ionosphere in the Brazilian sector shows significantly different behavior from that of the midlatitude sector.

The ionosphere has been studied extensively to support WAAS in the CONUS sector. The published literature discussing ionospheric corrections for WAAS in CONUS is extensive; see, e.g., [1–4]. Various alternative ionospheric correction algorithms have been presented (e.g., [5–7]). A potential application of WAAS algorithms to Brazil was recently investigated using simulated data [8]. The temporal and spatial variability of the low-latitude ionosphere was studied in the context of ionospheric storms by, e.g., [9–10], using a network of dual-frequency GPS receivers in Brazil. Investigating the possible application of the current WAAS algorithm using actual GPS data is the natural progression of the previous studies and therefore the main focus of this paper.

In this paper, we first review the estimation method used to solve for interfrequency biases (nuisance parameters) in the GPS satellites and receivers using a global network of 230 GPS sites to provide "ground truth" data for the analysis. Subsequently, we describe the WAAS planar fit algorithm used to estimate the vertical ionospheric range delay at fixed latitude/longitude locations, known as ionospheric grid points (IGPs). We examine the implications of using the currently adopted WAAS algorithm in Brazil and compare ionospheric range residuals using receivers in CONUS with those of Brazilian stations. We characterize a number of error sources affecting the computed ionospheric range delays.

GLOBAL IONOSPHERIC MAPPING (GIM) BIAS ESTIMATION STRATEGY

To provide ground-truth, we used the Global Ionospheric Mapping (GIM) software developed at the National Aeronautics and Space Administration's

NAVIGATION: *Journal of The Institute of Navigation*
Vol. 50, No. 3, Fall 2003
Printed in the U.S.A.

(NASA) Jet Propulsion Laboratory (JPL) [11] to compute high-precision slant ionospheric delay by removing the satellite and receiver differential biases from the ionospheric observables, generated from carrier-phase data adjusted to match the ionospheric delay based on dual-frequency pseudoranges. The estimation of the satellite and receiver biases is described here briefly.

Ionospheric measurements from a GPS receiver can be modeled with the well-known single-shell ionospheric model using the following observation equation [12–13]:

$$\mathrm{TEC} = \mathrm{M(h,E)}\sum_i C_i B_i(\mathrm{lat,lon}) + b_r + b_s \qquad (1)$$

where

- TEC is the slant total electron content measured by the linear combination of the GPS dual-frequency carrier-phase and pseudorange ionospheric observables, typically expressed in TEC units. One TEC unit (10^{16} electron/m^2) corresponds to about 0.163 m ionospheric delay at the L1 frequency.
- M(h,E) is the thin-shell mapping function for ionospheric shell height h and satellite elevation angle E (for the definition of the thin-shell geometric mapping function, see, e.g., [11, 14]).
- B_i(lat,lon) are horizontal basis functions (based on, for example, bicubic splines or bilinear interpolants) evaluated at the ionospheric pierce point (IPP)—the intersection of the ray path of a signal propagating from the satellite to the receiver with a thin spherical shell—located at latitude lat and longitude lon on the thin shell.
- C_i are basis function coefficients (real numbers).
- b_r, b_s are the satellite and receiver differential biases, assumed constant over periods of 24 h or more.

The dependence of vertical TEC on latitude and longitude is parameterized as a linear combination of the two-dimensional basis functions B_i, which are functions of solar-geomagnetic longitude and latitude [11]. (We note that the summation in equation (1) is over all basis functions B_i.) Using the carrier-phase–leveled ionospheric GPS observables, a Kalman filter simultaneously solves for the instrumental biases and the coefficients C_i, which are allowed to vary in time as a random walk stochastic process [15]. The basis functions currently used are based on a bicubic spline technique developed at JPL [16].

Although the main focus of this research is the comparison between CONUS and Brazilian sectors, we decided to use a global network of some 230 stations to solve for high-precision satellite and receiver differential biases that are used to correct the measurements. Research has shown that the most reliable satellite bias estimates can be achieved when using the data strength of a global network of GPS receivers instead of regional GPS networks [14]. We note that the WAAS system itself uses a similar estimation scheme for biases applied over the regional WAAS network.

WAAS PLANAR FIT IONOSPHERIC MODEL

In the currently implemented WAAS ionospheric real-time correction algorithm, the vertical ionospheric delay is estimated at each IGP by constructing a planar fit to a set of (bias-corrected) slant measurements projected to vertical:

$$\mathrm{TEC} = \mathrm{M(h,E)}[a_0 + a_1 d_E + a_2 d_N] \qquad (2)$$

where a_0, a_1, a_2 are the planar fit parameters, and d_E,d_N are the distances from the IGP to the IPP in the eastern and northern directions, respectively.

Each least-squares fit includes all IPPs that lie within a minimum fit radius surrounding the IGP. If the number of IPPs within this minimum radius is less than N_{min}, the fit radius R_{fit} is extended until it encompasses N_{min} points. In this study, we do not tabulate data when the fit radius is increased to its maximum value of R_{max} without having reached N_{min} points. Because of the high spatial variability of the ionosphere at low latitudes, R_{max} was chosen to be 500 km, which is significantly smaller than the value being used for WAAS (2100 km in the current implementation). When ionospheric spatial gradients are large, we expect smaller fit radii to provide higher accuracy (experience tuning the WAAS algorithms in CONUS tends to confirm this). The disadvantage of using smaller radii is that it lowers the number of points in the fit, which may lower the integrity of the corrections. However, the focus of this initial study is the relative accuracy of ionospheric corrections between low and midlatitudes. We wanted to obtain results as good as is practical with the planar fit at low latitudes, which suggests using small fit radii. We used the same 500 km value for R_{max} in our assessment of the residuals in CONUS.

In our WAAS estimation scheme (see equation (2)), we did not solve for the satellite and receiver differential biases. Instead, we used the GIM approach, outlined in equation (1), to solve for high-precision differential biases, and calibrated the ionospheric range measurements before applying equation (2). This approach is similar to that used in WAAS.

DATA ANALYSIS STRATEGY

In our data analysis, we treated every IPP data point as if it were collocated with a WAAS IGP (a so-called "pseudo IGP" approach). Subsequently, we applied the WAAS planar fit ionospheric model algorithm to estimate the vertical ionospheric delays at each of these IPPs, but excluding the particular IPP from the planar fit. Starting with the set of measurements that contributed to the planar fit, we then computed the residual difference between the slant measurements and the estimated slant delays based on the planar fit, projecting the vertical TEC from the planar estimate into the line of site using the WAAS thin-shell obliquity factor. This residuals analysis provides a measure of the performance of the planar fit algorithm in reproducing slant TEC for the user.

To investigate how ionospheric spatial gradients contribute to errors in the WAAS corrections in the CONUS and the Brazilian sectors, we looked at pairs of GPS receivers observing the same satellites at nearly identical elevation and azimuth angles. Vertical delay differences were computed after projecting the slant ionospheric range delay into the vertical. See the left panel of Figure 1.

We were also interested in determining the potential range errors introduced by using the WAAS thin-shell mapping function in Brazil. To that end, we analyzed measurements for which the IPPs were nearly collocated but differed in elevation angle. Mapping function errors were computed by taking the difference between the two slant ionospheric measurements, each projected to the vertical using the WAAS thin-shell mapping function. For an illustration, see the right panel of Figure 1.

DATASETS

For our test dataset, we chose a quiet and a storm day, March 30 and March 31, 2001, respectively, using GPS receivers from the Continuously Operating Reference Stations (CORS) network, maintained by the U.S. National Geodetic Survey [27], the International GPS Service (IGS) [18], and the Brazilian Network for Continuous Monitoring of GPS (RBMC). Figure 2 shows the Kp and DST indices for a period in 2001 indicating a major storm on March 31. The Kp and DST indices (for a description, see, e.g., [14, 19]) were obtained from the National Geophysical Data Center [19].

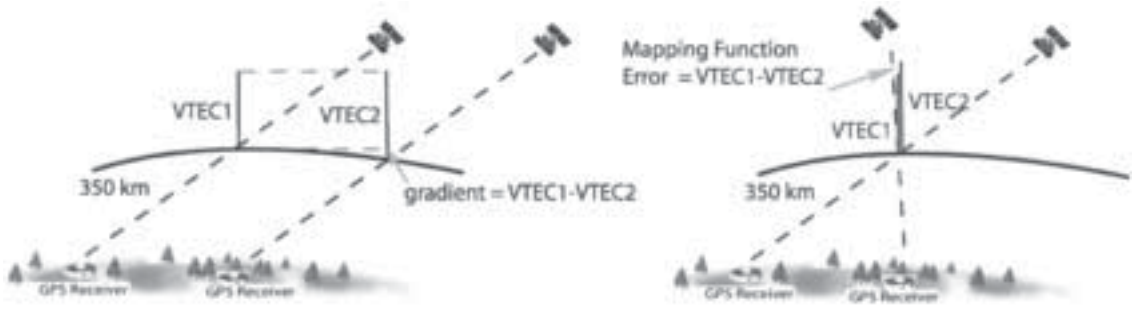

Fig. 1 – Left Panel: Illustration of Computing Ionospheric Delay Differences Versus Distance (gradient) for Separated Measurements with Similar Look Angles; Right Panel: Illustration of Computing Mapping Function Error. (Measurements with nearly collocated IPPs were differenced.)

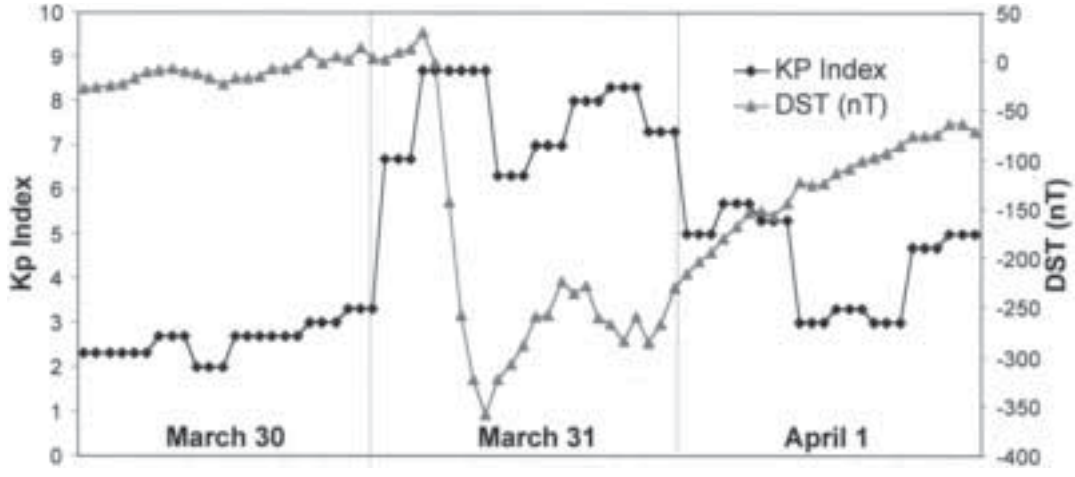

Fig. 2 – Behavior of Kp and DST Indices during the Focus Period in March (Negative excursions in DST indicate increased ring current in the earth's magnetosphere brought on by geomagnetic disturbances. Increases in the Kp index indicate enhanced geomagnetic activity at a number of globally distributed magnetic observatories.)

Figure 3 shows the global distribution of the GPS reference stations for March 31. The small dark solid circles represent the 230 sites that were used to provide unbiased line-of-site TEC ground-truth data. The larger circles indicate the CONUS and Brazilian sectors from which stations were used for the residual analysis.

ANALYSIS OF RESULTS

First we calibrated the satellite and receiver differential biases using the GIM method and data from the global network. Subsequently, we selected the GPS sites in Brazil and the same number of GPS sites in the CONUS sector to study the residuals when the same WAAS algorithm is applied to both low- and midlatitude sites.

Comparison of CONUS and Brazilian Planar-Fit Residuals for Quiet Day

We selected one station from CONUS (PRCO at Purcell, Oklahoma) and another in Brazil (UEPP at Sao Paulo, Brazil) to illustrate typical behavior of the slant ionospheric delays and residuals to the planar fit. (See Figure 3 for stations PRCO and UEPP, indicated with arrows.) Note that the residuals shown in Figure 4 (scale on the right) are all plotted in the slant domain. To compute residuals, the fitted vertical TEC value at an IPP location was converted to slant and differenced with the slant TEC measurement. We looked at several sites and concluded that PRCO and UEPP are representative for low- and midlatitude conditions.

Figure 4 reveals that slant-range ionospheric delays for CONUS range between 0 and 38 m for this period of high solar activity, whereas in the low-latitude sector, the highest values can be as much as 52 m (an elevation cutoff angle of 10 deg was used throughout this analysis). In the second Y axis, we also indicate the WAAS planar fit residuals (difference between slant measurement and fitted vertical delay converted to slant). For the geomagnetically quiet day, we find that WAAS planar fit slant residuals never exceed 2 m for CONUS, but reach as high as 8 m for station UEPP in Brazil.

The slant-range residuals are replotted in Figure 5, this time as a function of elevation angle, for CONUS (light) and Brazil (dark). It is interesting that the spatial variability of the equatorial ionosphere is so high that we cannot see a clear elevation angle dependence in the Brazilian residuals. However, the elevation angle dependence of these residuals is quite pronounced in CONUS. Generally, we would expect the residuals to grow with lower elevation angle since the additional path length through the ionosphere at lower elevations increases the range delay by up to a factor of 3.

Figures 4 and 5 show results for the quiet day of March 30. The subsequent day, March 31, turned out to be a day with a significantly disturbed ionosphere, corresponding to the largest geomagnetic storm of 2001.

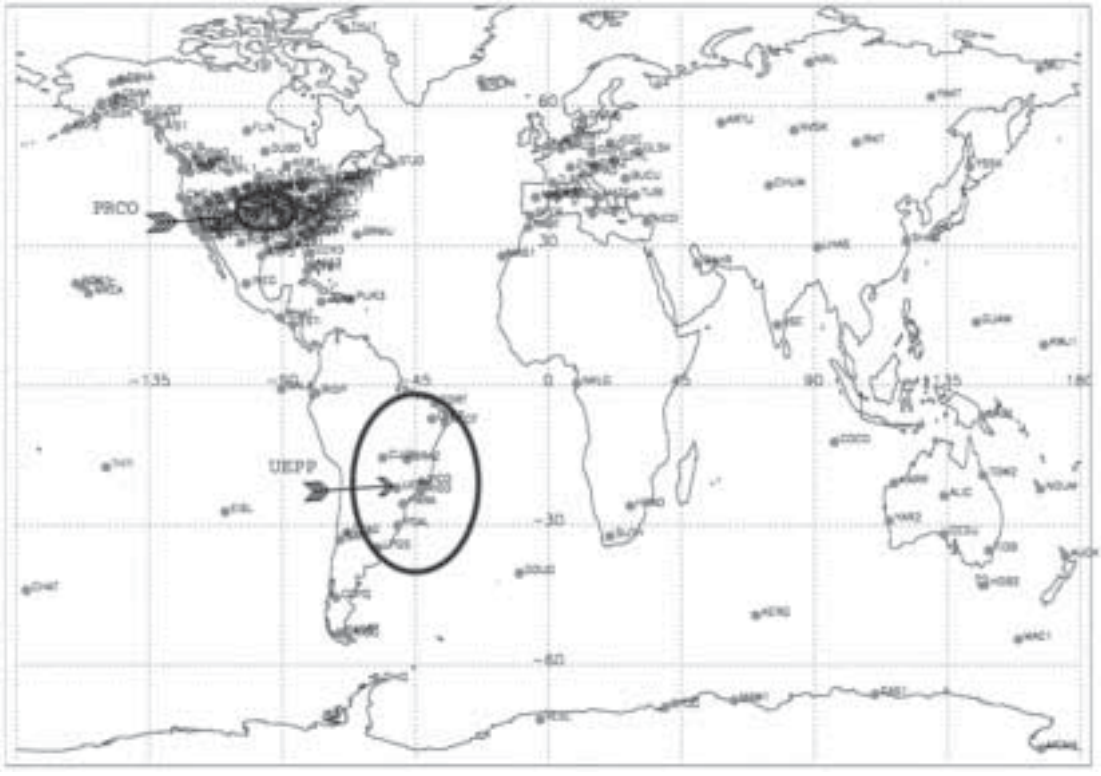

Fig. 3–Network of CORS, IGS, and RBMC Stations Processed for March 30–31, 2001

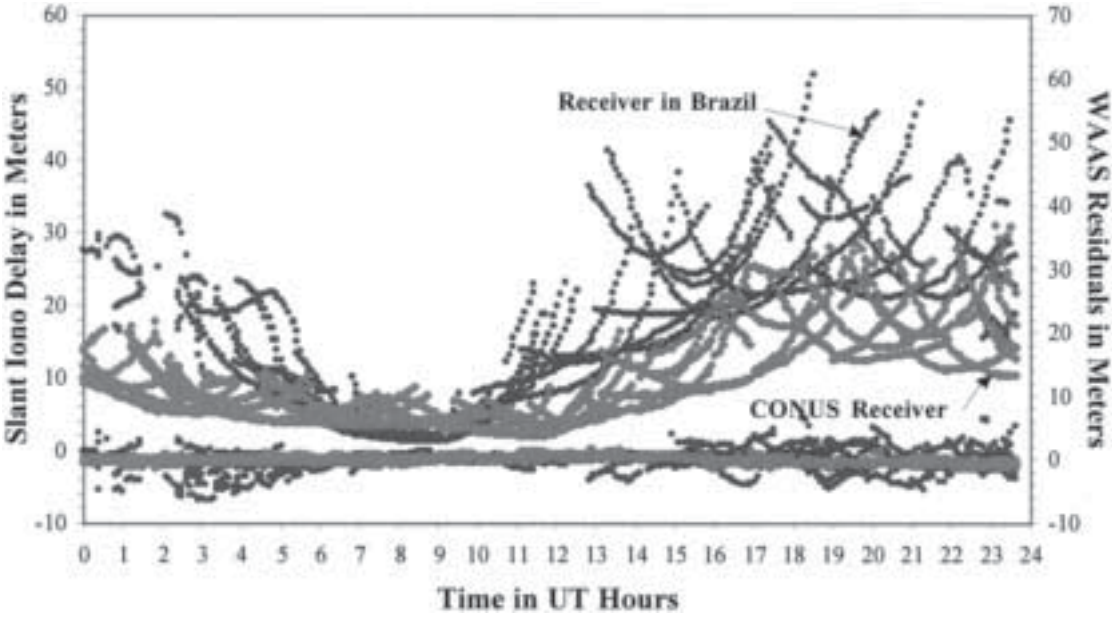

Fig. 4–Ionospheric Slant Delays for a Typical CONUS (light) and Brazilian (dark) Station for the Quiet Day, March 30, 2001 (Slant-range residuals to the planar fit are also shown.)

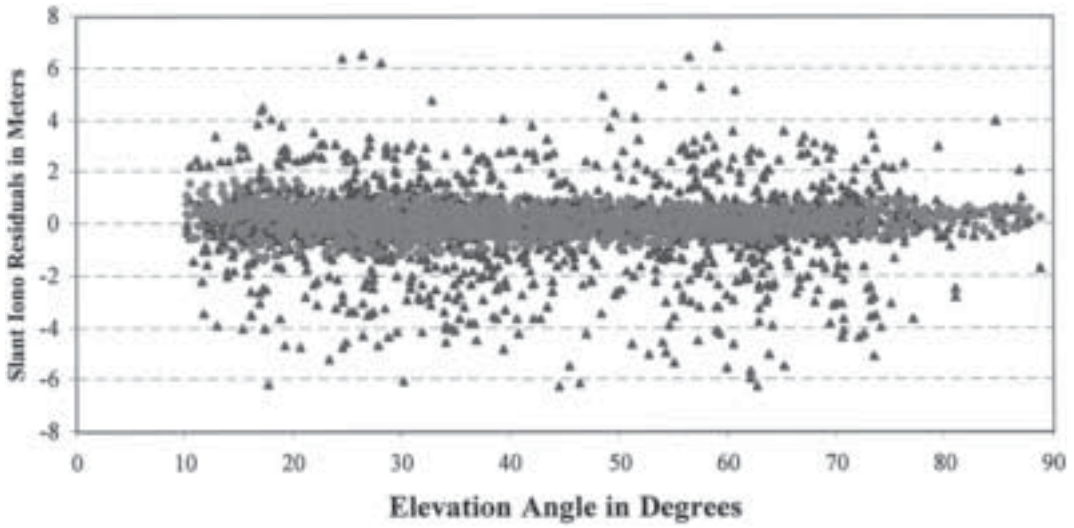

Fig. 5–Elevation Angle Dependence of WAAS Planar-Fit Residuals for a Typical CONUS (light) and Brazilian (dark) Station for a Quiet Day, March 30, 2001

In the following sections, we compare the ionospheric model behavior between quiet and storm conditions.

Differences in TEC between Quiet and Storm Days

To demonstrate the impact of storm activity, we generated differences using all 230 stations processed for each day. The differences were formed on an individual slant TEC measurement basis, i.e., differencing the measurements between the quiet and storm days, using the same receiver observing the same satellite on the subsequent day minus 4 min to observe exactly the same geometry (correction for sidereal rotation). We found interday TEC differences as large as 60 TEC units (9.6 m on L1) in the middle of the CONUS sector, possibly indicating the presence of storm-enhanced densities (SEDs) and depletions within CONUS [20]. It is worth pointing out that for the CONUS region, the differences turned out to be as high as they are for the Brazilian sector. However, since CONUS delays are generally much lower than those in Brazil, the relative impact of this storm in CONUS exceeded that in Brazil.

Comparison of Brazilian Residuals between Quiet and Storm Days

Figure 6 displays the Brazilian WAAS planar-fit residuals for both quiet and storm days. Note that

the behavior of the residuals is qualitatively similar. This suggests that the temporal and spatial variability of the equatorial anomaly may be masking the effects caused by the storm. This conclusion appears to be supported by the fact that we found similar delay differences between quiet and storm days in CONUS and Brazil. For both quiet and storm days, the magnitude of the Brazilian ionospheric residuals occasionally exceeded 18 m.

Comparison of CONUS Residuals between Quiet and Storm Days

The conclusion is slightly different when comparing the WAAS CONUS residuals between storm and quiet days. In Figure 7, it is evident that the storm contributed to higher residuals by more than a factor of 3 during universal time (UT) hours 16 to 23 (local time [LT] corresponds to UT minus 3 h). Slant residual magnitudes barely exceed 2 m for the quiet day, but reach nearly 8 m for the storm day.

Histogram of All Planar-Fit Residuals for Storm Day

We also computed histograms of all residuals for the CONUS and Brazilian sectors. In Figure 8, note the difference in the shape of the distributions. The distribution of the Brazilian residuals is more similar to a double exponential and deviates from a typical Gaussian-shaped distribution. Similar conclusions are reached in [8] using simulated data points from the ionospheric models PIM and LowLat. We found the largest residual values of 18 and 7.5 m for the

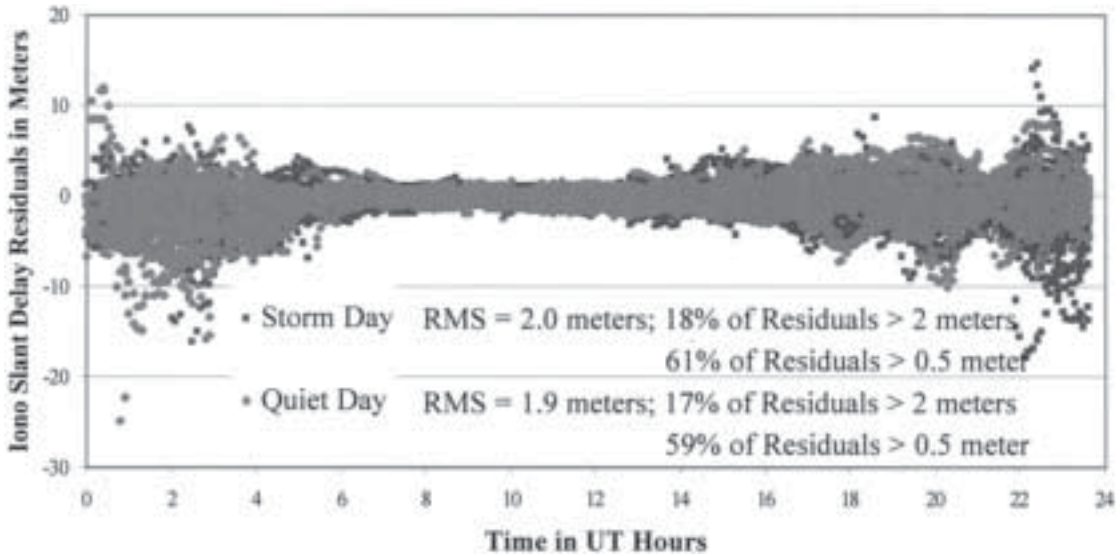

Fig. 6–Brazilian Planar-Fit Slant-Range Residuals for Quiet (light) and Storm (dark) Days Using 10 Stations

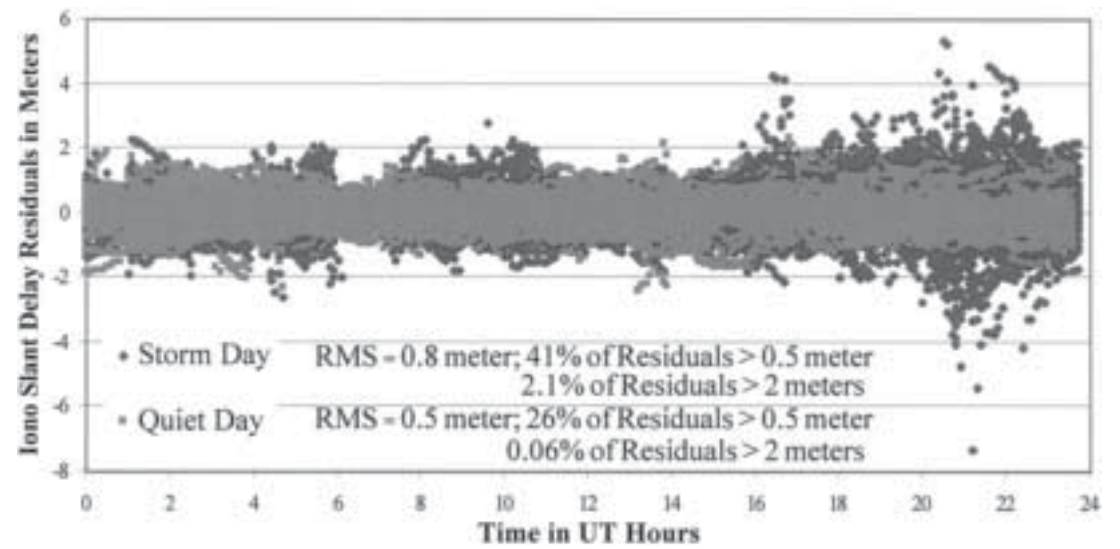

Fig. 7–CONUS Planar-Fit Slant-Range Residuals for Quiet (light) and Storm (dark) Days Using 10 CONUS Stations

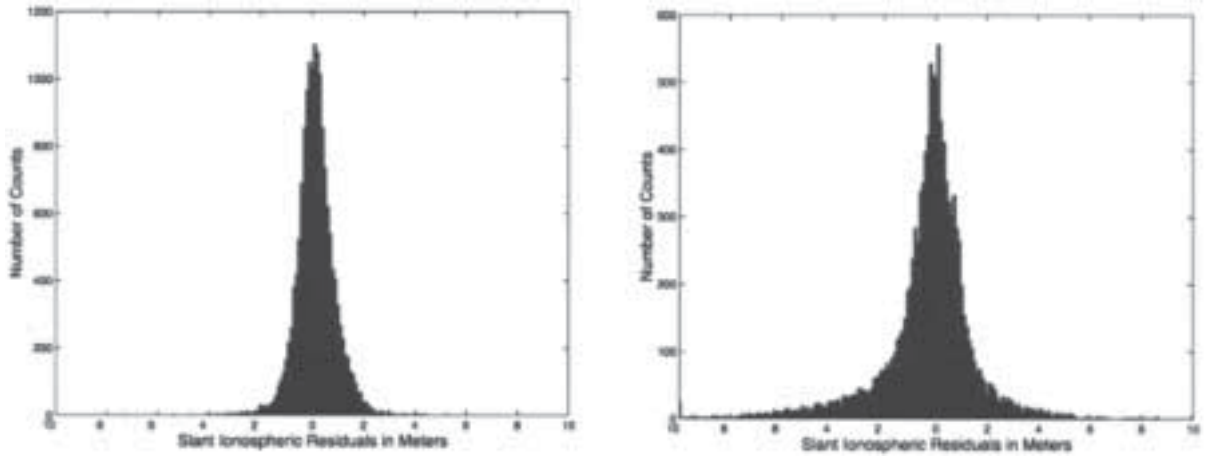

Fig. 8–Histograms of Storm-Time Slant Delay Residuals for the CONUS (left panel) and Brazilian (right panel) Stations

Brazilian and CONUS regions, respectively. In Figure 8, the same abscissa range (−10 to 10 m) for CONUS and Brazil is used to reveal the different shape of the distributions. Neither distribution appears to be Gaussian, probably as a result of highly varying ionospheric conditions that cannot be described by a simple Gaussian distribution. We note that careful interpretation is required when binning the residuals data for a single day while conditions are varying throughout the day, as occurs when a storm is present.

Characterizing WAAS Ionospheric Delay Differences

In equation (2), it was shown that the WAAS algorithm estimates a constant term and slope terms in the east-west and north-south directions. To evaluate the WAAS planar fit performance further, we decided to take a closer look at the two gradient parameters estimated in the WAAS planar fit algorithm (equation 2). We generated ground truth by selecting pairs of stations observing the same satellites at nearly identical elevation and azimuth angles. We computed vertical delay gradients by differencing the vertical TEC from these stations and tabulating the distance between them. The slant delays were converted to vertical using the WAAS obliquity scaling factor (thin shell at 350 km). For additional explanation and illustration (left panel of Figure 1), see the section on data analysis strategy.

Delay Difference between Two Receivers: Time Series at Midlatitude for the Quiet Day

One such example is shown in Figure 9, which displays the difference between measured and estimated ionospheric delay for two receivers observing the same satellite at similar azimuth and elevation

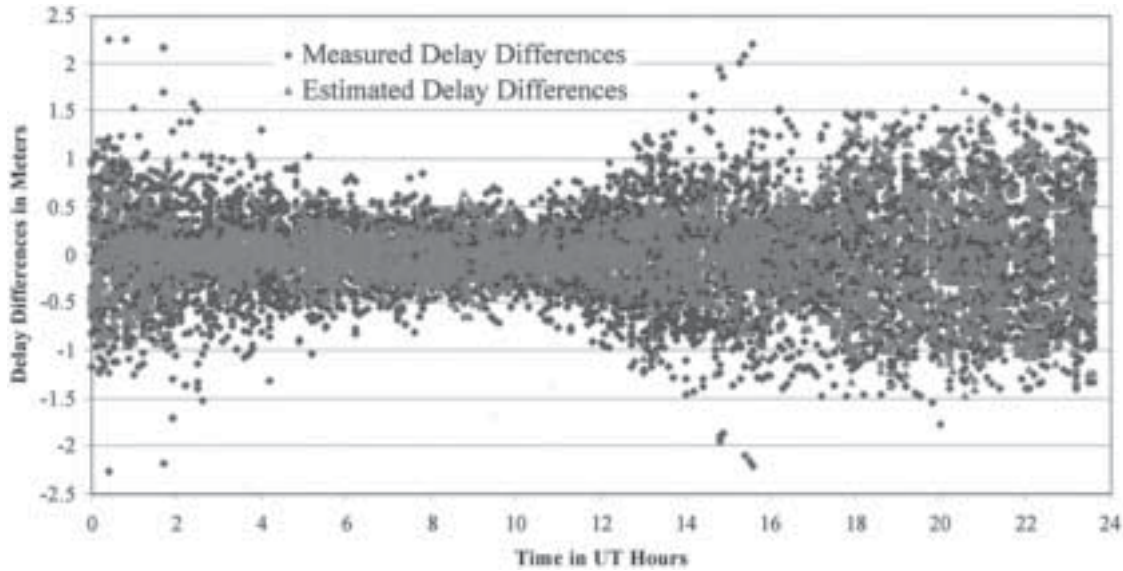

Fig. 9–Measured (dark) and Estimated (light) WAAS Vertical Delay Differences for Nearby Receivers (measurement spacing < 500 km) for a CONUS Quiet Day

angle. After limiting the maximum separation between IPPs to 500 km, we found that the delay differences in CONUS could reach nearly 2.5 m over 500 km for the quiet day. Figure 9 clearly shows the diurnal variation of the delay differences. The estimated delay differences usually overlap the measured values, indicating qualitatively that the actual delay differences are usually well modeled by the fitted planar variation. However, we note larger discrepancies during the dawn and dusk hours, when the temporal and spatial variability of the ionosphere is generally at its peak.

Delay Difference Time Series at Midlatitude for the Storm Day

Figure 10 displays the measured and estimated delay differences for the storm day, March 31. The increased differences due to the storm are quite evident starting at about 16 h UT (corresponding to about 13 h LT). Measured delay differences during the storm (over distances less than 500 km) reach as high as 6.5 m. This is an increase of nearly a factor of 3 compared with the quiet conditions as depicted in Figure 9 (note the different vertical scales in the two figures). Not surprisingly, during the storm hours we also find larger discrepancies between the measured and estimated delay differences (shown in the figure as the vertical distance between the dark dots and corresponding light dots). The largest difference between measured and estimated gradient is 5 m at 21 h UT over a distance of 480 km.

Delay Difference Distance Dependence at Midlatitude for the Quiet and Storm Days

We also investigated the measured and estimated delay differences as a function of the distance between two observations at nearly identical elevation and azimuth angles. We evaluated the delay differences in terms of longitudinal ($a_1 d_E$) and latitudinal ($a_2 d_N$) components, as estimated by the planar fit algorithm in equation (2). As expected, the latitudinal (north-south) components dominate the delay differences. For the quiet day, we found that ionospheric gradients along the north-south direction did not exceed 0.5 m over 100 km. Some of the larger differences between the measured and estimated delay differences correspond to dawn and dusk periods, as was shown in Figure 9. For the storm day, we found that the north-south gradients were bounded by 1.2 m over 100 km, which represents an increase of more than a factor of 2 compared with the quiet-day conditions. We also found an increased contribution of the longitudinal gradient, suggesting more-complex structures in the midlatitude ionosphere as we had already noticed a significant increase in the RMS of residuals compared with the quiet-day conditions.

Elevation Angle Times Series

Figure 11 plots the delay differences as a function of elevation angle. It appears to indicate no elevation angle dependence, which is what we expected, providing evidence that the selection of pairs of stations with nearly identical elevation and azimuth angles was performed with sufficiently tight tolerances (elevation angle tolerance less than 2 deg, azimuth angle tolerance less than 30 deg). To obtain sufficient numbers of observation pairs, the elevation and azimuth tolerances should not be overly restrictive. Stringent elevation and azimuth angle tolerances

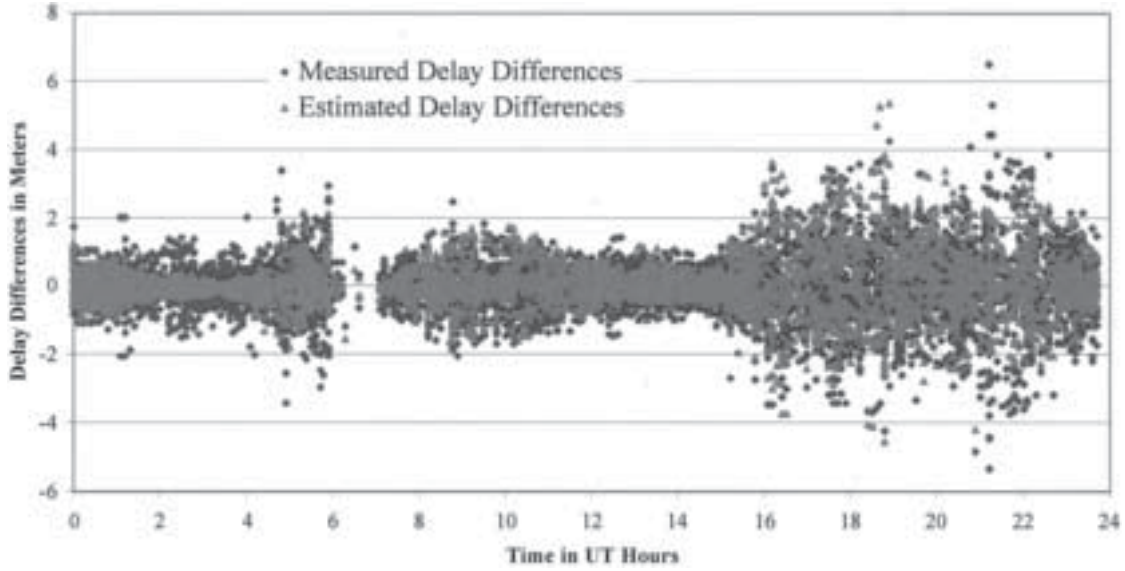

Fig. 10–Measured (dark) and Estimated (light) Vertical Delay Differences for the CONUS Storm Day

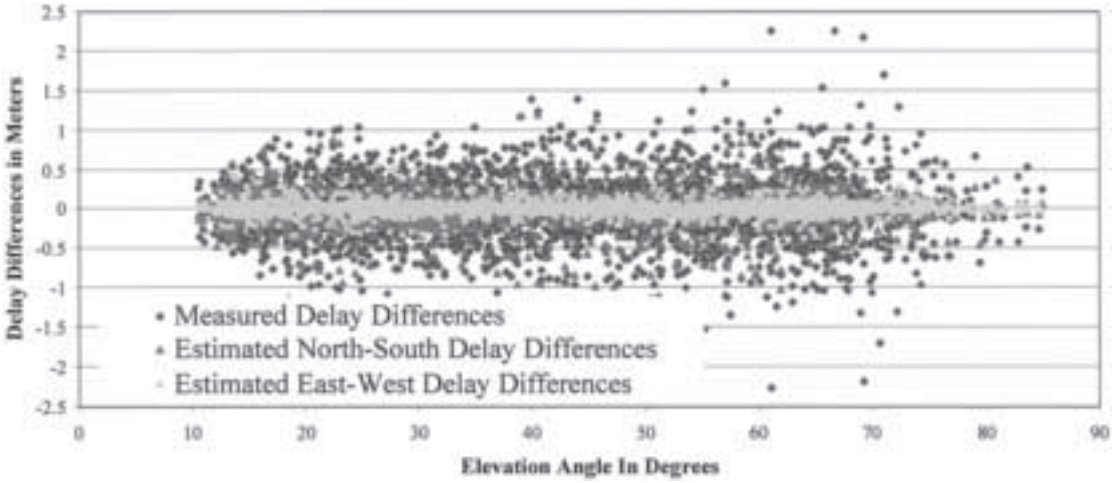

Fig. 11–Elevation Angle Dependence of the Delay Differences for the Quiet Day, March 30, 2001 (Weak dependence suggests that the azimuth/elevation tolerances are not too loose.)

result in a small number of observation pairs, while observations with loose tolerances would no longer represent the same geometry.

Delay Difference Time Series at Low Latitude for the Quiet and Storm Days

Figure 12 shows the measured and estimated vertical delay differences for the Brazilian sector during the quiet day. The discrepancy between the measured and estimated delay differences is more evident than for the CONUS sector. Even for the quiet day (see Figure 12), we detect large discrepancies in the measured and estimated delay differences during 20 to 06 h UT. The overall RMS of measured and estimated range delay differences was 1.9 m. Note that the current distribution of GPS sites in Brazil results in a smaller number of observations meeting the criterion of two observations being at nearly the same elevation and azimuth angles, compared with the better spatial distribution of CONUS receivers.

After performing the same comparison for the storm day, we found no evidence of a major storm. The overall structure of the delay differences is very similar to that for the quiet day; the RMS of slant residual differences between measured and estimated values is 2.0 m.

To obtain a complete picture, we also investigated the delay differences as a function of distance between the two points used in the gradient calculation. For the quiet and storm days, we observed similar delay differences, as high as 10 m over 500 km (2 m over 100 km).

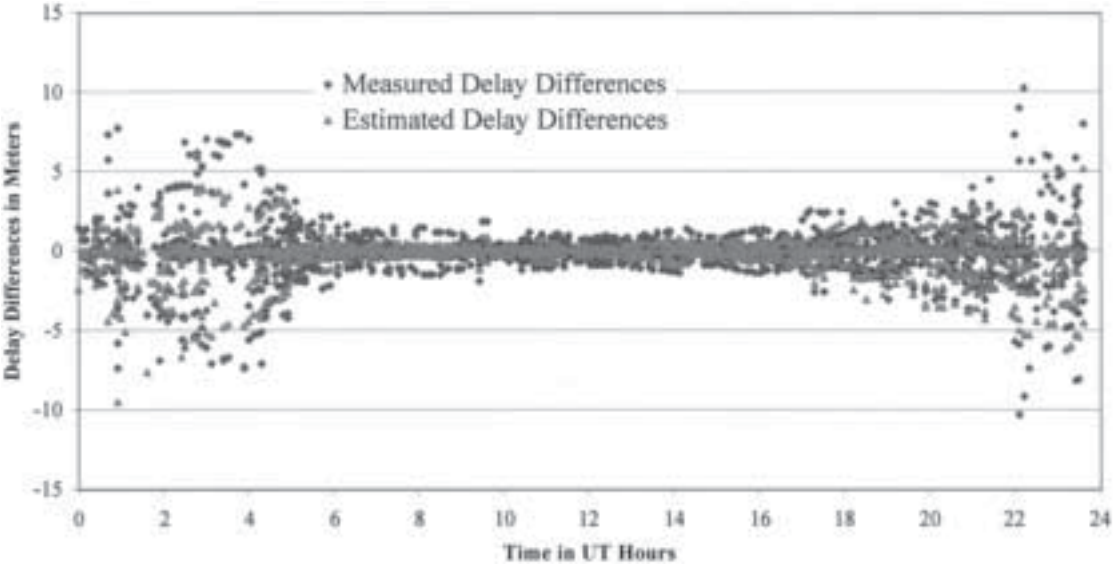

Fig. 12–Measured (dark) and Estimated (light) Vertical Delay Differences for Brazil During the Quiet Day

Mapping Function Error

As another potential error source, we explored the errors introduced by the thin-shell ionospheric mapping function. The idea is to find pairs of observations from different receivers with nearly collocated IPPs (for illustration, see the right panel of Figure 1). If the elevation mapping function contains no errors, the two slant observations should provide identical vertical range delays. In fact, mapping function errors are present, and assessed by projecting the two slant observations into the vertical using the respective elevation angles and subsequently taking the difference between the two nearly collocated vertical estimates. Figure 13 shows the elevation angle dependence of the mapping function errors for CONUS and Brazilian (elevation angle of the pseudo IGP used for plotting). For CONUS, the errors never exceed 2 m; for the Brazilian sector, they can exceed 8 m.

The highest value for mapping function error (as high as 8 m) is consistent with the maximum error of −13.4 m obtained in [8] using simulated data down to 5 deg elevation cutoff angle. In our study, we used a 10 deg elevation cutoff angle. The statistics we computed refer to mapping function errors in vertical delay. One would need to multiply the errors by an average factor of about 2 (a factor of 3 at 10 deg elevation angle) to compute slant delay errors due to the mapping function.

Implications for Lateral Navigation/Vertical Navigation (LNAV/VNAV) Availability

We investigated ionospheric range errors in the midlatitude CONUS and low-latitude Brazilian sectors for the quiet and storm days. Based on this limited dataset, we found that using a tuned variant of the WAAS planar fit algorithm enabled us to achieve ionospheric slant delay residuals of better than 0.5 m RMS for the quiet day and 0.8 m RMS for the storm day in CONUS. For the Brazilian sector, we obtained RMS residuals of 1.9 m in slant delay for the quiet day and 2.0 m for the storm day.

The quiet-day CONUS results are reasonably consistent with what has been observed in previous analyses of ionospheric residuals to the planar fit for quiet conditions [3]. Residuals in Brazil are larger by approximately a factor of 4 on average. This finding has major implications for the availability of the initial WAAS Lateral Navigation/Vertical Navigation (LNAV/VNAV) service. The user determines, in real time, the level of navigation service available based on the broadcast grid ionosphere vertical errors (GIVEs) and other information. GIVE values represent 3.29σ bounds on vertical ionosphere range error at each ionospheric grid point. Service volume model studies for WAAS have shown that high availability of LNAV/VNAV service is possible when a significant majority of the broadcast GIVEs are in the range 3–6 m. This performance is expected for WAAS.

At low latitudes, the GIVEs must be increased to cover the larger ionospheric range errors expected. Increased planar fit residuals by a factor of 4 are likely to result in a substantial number of GIVEs above 6 m. As a result of GIVE quantization in the broadcast message, computed GIVEs above 6 m are transmitted as 15 m bounds to the user. It is clear that LNAV/VNAV service will be unavailable if several of the user's satellite links are associated with GIVEs of 15 m or more.

We expect that the WAAS planar fit algorithm applied to Brazil will result in significantly reduced availability of the LNAV/VNAV service, particularly near solar maximum during daytime and evening hours. Additional factors, such as the possible presence of plasma bubbles observed in the equatorial region [9], will further contribute to much larger GIVE values in Brazil compared with CONUS.

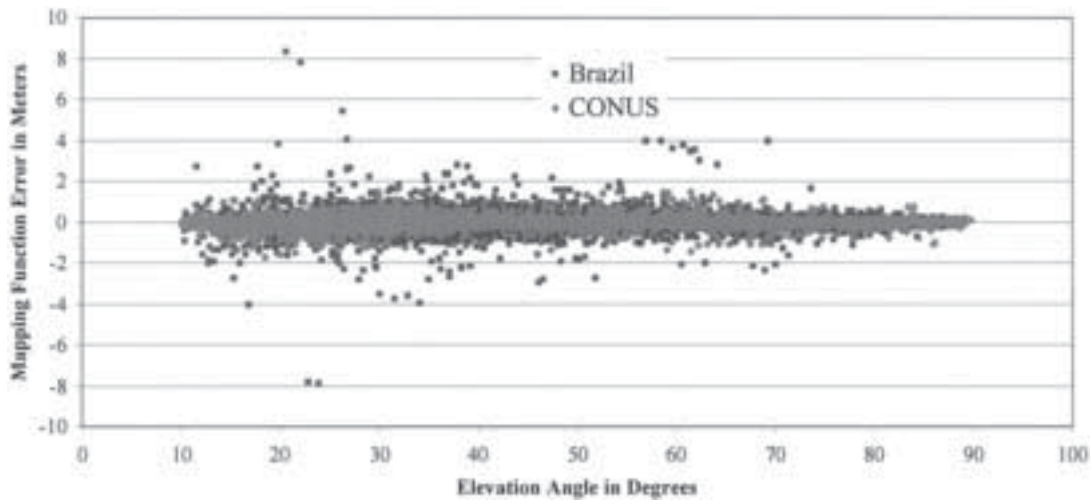

Fig. 13–Mapping Function Errors for CONUS (light) and Brazil (dark) as a Function of Elevation Angles

CONCLUSIONS AND FUTURE RESEARCH

In this paper, we have compared the performance of the WAAS ionospheric planar-fit correction algorithm in the CONUS and Brazilian sectors using a limited dataset based on quiet and storm days from recent high-solar-activity periods. To perform this comparison, we used data from a network of dual-frequency GPS receivers in the midlatitude CONUS and Brazilian sectors. Unbiased line-of-sight TEC ground-truth data were generated using JPL's GIM software. Using the truth data, the WAAS planar-fit algorithm was evaluated by treating each observation as representing a WAAS IGP and computing the planar fit estimate for that IGP after excluding it from the fit.

We found slant ionospheric range delays of up to 30 m for daytime CONUS and as high as 60 m for Brazil. For the quiet day, we obtained WAAS planar-fit residuals of less than 2 m (0.5 m RMS) for CONUS and usually less than 15 m (1.9 m RMS) for Brazil. For the storm day, the WAAS planar fits resulted in residuals of less than 8 m (0.8 m RMS), compared with the residuals for Brazil of up to 18 m (2.0 m RMS). It is interesting to see that the storm had a small impact on the planar-fit residuals in the Brazilian sector as compared with quiet conditions. However, the storm effect was more pronounced in the CONUS region.

For CONUS, we found that ionospheric gradients, averaged over distances of a few hundred kilometers, were no larger than 0.5 m per 100 km for the quiet day, and no larger than 1.2 m over 100 km for the storm day. For Brazil, we observed gradients as large as 2 m over 100 km both for quiet and storm days. Studies reported in [9] found similar or even larger gradients in Brazil, associated with plasma bubbles typically appearing after sunset during solar maximum.

Mapping of slant observations to the vertical occasionally resulted in errors of about 8 m (vertical) in Brazil. In CONUS, these errors never exceeded 2 m on the processed day.

This investigation addressed only some of the difficulties users will face in the Brazilian sector in employing the current WAAS algorithm. It appears that the inherent spatial variability of the ionosphere is driving the residual errors seen at low latitudes. Other influential factors, such as bubbles and plumes, have not been addressed in this paper. Since the datasets we analyzed represented one day each of high-solar-activity quiet and storm conditions, the results cannot be construed as conclusive. These preliminary results may, however, be considered an approximation of the upper bounds for conditions of medium and low solar activity.

We are currently investigating alternative algorithms to augment or replace the WAAS algorithm in Brazil. This alternative will include fitting higher-order surfaces to the data. Initial assessment of fitting a quadratic surface to the data revealed only a marginal improvement in accuracy.

In addition to large ionospheric delays and gradients in the equatorial region, users will also be exposed to 15–20 m level large depletions or "bite-outs" due to plasma bubbles [9]. We are planning to evaluate these effects and determine the density of ground stations necessary to detect these structures so that full integrity of the corrections is maintained.

Previous studies of ionospheric decorrelation have relied on so-called WAAS "supertruth" data derived from collocated GPS receivers for robust detection of anomalies in the data. In the absence of Brazilian supertruth data, this research was conducted using dual-frequency GPS data from CORS, IGS, and Brazilian sites with no redundant observations available.

With no redundancy, robust data-editing algorithms were applied to remove outliers, but it is possible that some valid data was rejected or that marginally poor data was accepted. Preprocessing of the raw data was conducted carefully to ensure that the data-editing algorithm would not eliminate large numbers of observations. Consideration of the number of accepted points between the two days suggests that data editing did not play a significant role in this study. Based on our analyses, we expect that data editing played at most a minor role in the conclusions drawn thus far. This issue will be investigated further in the future.

ACKNOWLEDGMENTS

This research was performed at the Jet Propulsion Laboratory/California Institute of Technology under contract to the National Aeronautics and Space Administration and the Federal Aviation Administration. We greatly appreciate the help of Dr. Eurico de Paula and Mariangel Fedrizzi (both at the Instituto Nacional de Pesquisas Espaciais, INPE) in providing us with the GPS data for Brazil.

Based on a paper presented at The Institute of Navigation's ION GPS-2002, Portland, Oregon, September 2002.

REFERENCES

1. Enge, P., T. Walter, S. Pullen, C. Kee, Y. C. Chao, and Y. J. Tsai, *Wide Area Augmentation of the Global Positioning System*, Proceedings of the IEEE, Vol. 84, 1996, pp. 1063–88.
2. WAAS MOPS, *Minimum Operational Performance Standards for Global Positioning System/Wide Area Augmentation System Airborne Equipment*, RTCA Inc. Document No. RTCA/DO-229B, October 6, 1999, p. 225.

3. Walter, T., A. Hansen, J. Blanch, P. Enge, T. J. Mannucci, X. Pi, L. Sparks, B. Iijima, B. El-Arini, R. Lejeune, M. Hagen, E. Altschuler, R. Fries, and A. Chu, *Robust Detection of Ionospheric Irregularities*, Proceedings of The Institute of Navigation's ION GPS-2000, Salt Lake City, UT, September 11–14, 2000.
4. Sparks, L., A. Komjathy, and A. J. Mannucci, *Sudden Ionospheric Delay Decorrelation and Its Impact on WAAS*, Proceedings of the 10th International Ionospheric Effects Symposium, May 7–9, 2002.
5. Hansen, A. J., T. Walter, and P. Enge, *Ionospheric Correction Using Tomography*, Proceedings of The Institute of Navigation's ION GPS-97, Kansas City, MO, September 16–19, 1997, pp. 249–57.
6. Sparks, L., B. A. Iijima, A. J. Mannucci, X. Pi, and B. D. Wilson, *A New Model for Retrieving Slant TEC Corrections for Wide Area Differential GPS*, Proceedings of The Institute of Navigation's National Technical Meeting, Anaheim, CA, January 26–28, 2000, pp. 464–74.
7. Blanch, J., T. Walter, and P. Enge, *Application of Spatial Statistics to Ionosphere Estimation for WAAS*, Proceedings of The Institute of Navigation's National Technical Meeting, San Diego, CA, January 28–30, 2002.
8. Klobuchar, J. A., P. H. Doherty, M. Bakry El-Arinim, R. Lejeune, T. Dehel, E. R. de Paula, and F. S. Rodriges, *Ionospheric Issues for a SBAS in the Equatorial Region*, Proceedings of the 10th International Ionospheric Effects Symposium, May 7–9, 2002.
9. Dehel, T. and M. Corbelli, *Brazilian Test Bed: Ionospheric Analysis*, Presented at the ATN/GNSS CAR/SEM Seminar, Varadero, Cuba, May 6–9, 2002, http:/ /www.icao.int/nacc/meetings/atngnss2002/gnss_71b2_brazil.pdf.
10. Fedrizzi, M., R. B. Langley, A. Komjathy, M. C. Santos, E. R. de Paula, and I. J. Kantor, *The Low-Latitude Ionosphere: Monitoring Its Behavior with GPS*, Proceedings of The Institute of Navigation's ION GPS-2001, Salt Lake City, UT, September 11–14, 2001.
11. Mannucci, A. J., B. D. Wilson, D. N. Yuan, C. H. Ho, U. J. Lindqwister, and T. F. Runge, *A Global Mapping Technique for GPS-Derived Ionospheric Total Electron Content Measurements*, Radio Science, Vol. 33, 1998, pp. 565–82.
12. Mannucci, A. J., B. A. Iijima, L. Sparks, X. Pi, B. D. Wilson, and U. J. Lindqwister, *Assessment of Global TEC Mapping Using a Three-Dimensional Electron Density Model*, Journal of Atmospheric and Solar Terrestrial Physics, Vol. 61, 1999, pp. 1227–36.
13. Komjathy, A., B. D. Wilson, T. F. Runge, B. M. Boulat, A. J. Mannucci, L. Sparks, and M. J. Reyes, *A New Ionospheric Model for Wide Area Differential GPS: The Multiple Shell Approach*, Proceedings of The Institute of Navigation's National Technical Meeting, San Diego, CA, January 28–30, 2002.
14. Komjathy, A., *Global Ionospheric Total Electron Content Mapping Using the Global Positioning System*, Ph.D. Dissertation, Department of Geodesy and Geomatics Engineering Technical Report No. 188, University of New Brunswick, Fredericton, New Brunswick, Canada, 1997, p. 248.
15. Iijima, B. A., I. L. Harris, C. M. Ho, U. J. Lindqwister, A. J. Mannucci, X. Pi, M. J. Reyes, L. C. Sparks, and B. D. Wilson, *Automated Daily Process for Global Ionospheric Total Electron Content Maps and Satellite Ocean Altimeter Ionospheric Calibration Based on Global Positioning System*, Journal of Atmospheric and Solar-Terrestrial Physics, Vol. 61, 1999, pp. 1205–18.
16. Lawson, C., *A Piecewise C2 Basis for Function Representation over a Surface of a Sphere*, JPL Internal Document, 1984.
17. CORS, *Continuously Operating Reference Stations*, http:/ /www.ngs.noaa.gov/CORS/ [accessed August 10, 2002].
18. IGS, *International GPS Service*, http://igscb.jpl.nasa.gov/ [accessed September 5, 2002].
19. NGDC, *National Geophysical Data Center, Geomagnetic Data Base*, ftp://www.ngdc.noaa.gov/STP/ GEOMAGNETIC_DATA/INDICES/ [accessed September 2002].
20. Foster, J. C., P. J. Erickson, A. J. Coster, J. Goldstein, and F. J. Rich, *Ionospheric Signatures of Plasmaspheric Tails*, Geophysical Research Letters, Vol. 29, No. 15, 2002.